

Cell–cell communication by quorum sensing and dimension-reduction

Johannes Müller · Christina Kuttler ·
Burkard A. Hense · Michael Rothballer ·
Anton Hartmann

Received: 26 August 2005 / Revised: 12 June 2006 /
Published online: 5 August 2006
© Springer-Verlag 2006

Abstract Several bacterial taxa change their behavior if the population density exceeds a certain threshold. This phenomenon is the consequence of a communication system between the bacteria and is called quorum sensing (QS). Up to now, this phenomenon is mostly modeled at population level. However, new experimental techniques allow for single cell analysis. We introduce a modeling approach for the description of this QS system, including a discussion of the regulatory network and its bistable behavior. Based on this single-cell model we develop and analyze a spatially structured model for a cell population. Special attention is given to the scaling behavior w.r.t. the cell size (leading to an approximation theorem for stationary solutions) and its consequences for the interpretation of cell communication (QS versus diffusion sensing). Concluding, we apply the modeling approach to spatially structured experimental data.

Ch. Kuttler and J. Müller would like to dedicate this work to K.P. Haderler, who not only introduced us to the fascinating field of mathematical biology, but also offered friendship and help at so many occasions.

J. Müller (✉)
Centre for Mathematical Sciences, Technical University Munich, Boltzmannstr. 3,
85748 Garching/Munich, Germany
e-mail: johannes.mueller@gsf.de

Ch. Kuttler · B. A. Hense
Institute of Biomathematics and Biometry, GSF - National Research Center for Environment
and Health, Ingolstädter Landstr. 1, 85764 Oberschleißheim, Germany

M. Rothballer · A. Hartmann
Institute of Soil Ecology, Department of Rhizosphere Biology, GSF - National Research Center
for Environment and Health, Ingolstädter Landstr. 1, 85764 Oberschleißheim, Germany

Keywords Quorum sensing · Single cell analysis · Bistability Dimension reduction · Partial differential equation

Mathematics Subject Classification (2000) 92C15 · 35A35

1 Introduction

For an increasing number of bacterial taxa an intra- (and inter-) species communication system called quorum sensing (QS) is described [2,6,15,29,30]. QS is based on the continuous production of usually small amounts of signaling molecules which are released into the environment and can be sensed by the bacteria. The extracellular concentration depends on the cell density. When a critical signal molecule concentration is exceeded, this initiates a cellular response, usually by induction of gene transcription. This concentration is thought to be mainly achieved by reaching a critical cell density (=quorum). However, the relevance of other mechanisms as diffusion sensing (critical concentration threshold is exceeded if the diffusible area around a cell is sufficiently restricted, e.g., in pores) is also discussed [18].

QS was first described in *Vibrio fischeri*, a marine bacterium. *V. fischeri* occurs free-living in low concentration as well as in specialized light organs in some squid and fish species [6,21]. In the light organ (or in laboratory cultures) the bacteria bioluminesce blue–green light at high cell densities. The regulation is based on *N*-(3-oxohexanoyl)-L-homoserine lactone (3OC6HSL) [5]. 3OC6HSL is a member of the acyl homoserine lactone (AHL) family. AHLs are reported to act as QS signaling molecules in many gram negative bacteria, where they regulate a number of different processes [2,30]. *V. fischeri* is a suitable organism for studying QS as it is cultivable in vitro and in vivo (e.g., in squids), the QS reaction (bioluminescence) can easily be analyzed and it is possible to manipulate the organisms genetically. Therefore, *V. fischeri* presents the best investigated QS system and thus can be regarded as a model organism for the understanding of QS regulation. It turns out that the underlying gene regulation network implementing QS is quite similar across different taxa. Receptor molecules bind the signaling substance and subsequently polymerize [6,30]. These polymers bind to promoters and induce transcription of QS-cassettes which code (among other genes that code e.g., luminescing substances) for the proteins that produce the signaling substance and induce transcription. This results in a positive feedback loop. Due to the polymerization of the complex signaling substance / receptor molecule, the system develops a bistable behavior – this feedback acts as a genetic switch which is activated by a certain density of the signaling substance.

Classical experiments consider a homogeneous population in an aqueous suspension, where bacterial populations grow in a well stirred batch type reactor [8,9,16,17]. Once the population density has reached a critical threshold, the luminescence of the population increases suddenly by several magnitudes. Only recently, the experimental techniques have been improved. By now, it is

possible to obtain informations about single cells [24]. Molecular biology techniques facilitate the introduction of plasmids harboring genes for fluorescence marker molecules, which are expressed if a certain AHL threshold is exceeded. By confocal laser scanning microscopy (CLSM), the state and location of single cells can be obtained [7].

These data that allow for single cell analysis bear a new challenge for the mathematical evaluation. Until now, spatial models only consider the density of cells in different states. These models have been successfully applied to data [31, 28] and it is possible to perform a bifurcation analysis [4]. A special case of single cell models is developed in [10]. There, the situation of a single bacterium (*Staphylococcus aureus*) inside an endosome is considered which uses signal molecules for diffusion sensing. In this work we present a model that describes a population of single cells communicating by the QS-mechanism. This model assumes the form of a linear parabolic differential equation in the space outside the cells. The cells themselves are represented by nonlinear ordinary differential equations that reflect the basic structure of the genetic network. The parabolic partial differential equation is coupled with the ODEs via mixed boundary conditions at the cell surface (Sect. 2). In Sect. 3 we derive some analytic results for the long time behavior. The most important one indicates that trajectories starting from very small or from very large initial conditions tend to stationary states. Consequently, the present work focuses on stationary states. It is not possible to obtain stationary solutions directly. The key observation here is the fact that the cells are quite small compared to their distance. Rescaling arguments lead to an approximative equation, where cells are represented as inhomogeneities on the right hand side of the partial differential equation (assuming the form of point masses), while the domain of the PDE is the complete \mathbb{R}^3 . We are then able to solve the partial differential equation analytically and reduce the stationary problem to a finite system of (nonlinear) algebraic equations. An approximation theorem is proven. As an illustration of the possibility to apply this theory we (very briefly) discuss data from CLSM and their analysis (Sect. 4).

Though in the present work a lot of restrictive assumptions are made (e.g., cells are balls, the diffusion coefficient of the signaling substance is constant, the approximation handles only stationary states), we expect that the fundamental principles can be transferred to more complex cases. Also other communication systems using diffusible signaling substances but different genetic networks can be described in a similar way and the techniques developed here may be transferred and adapted.

2 The model

2.1 Within a cell: the pathway

The regulation pathways implementing QS by AHL are quite similar in most bacteria. Minor changes in the biochemical behavior of involved homologue

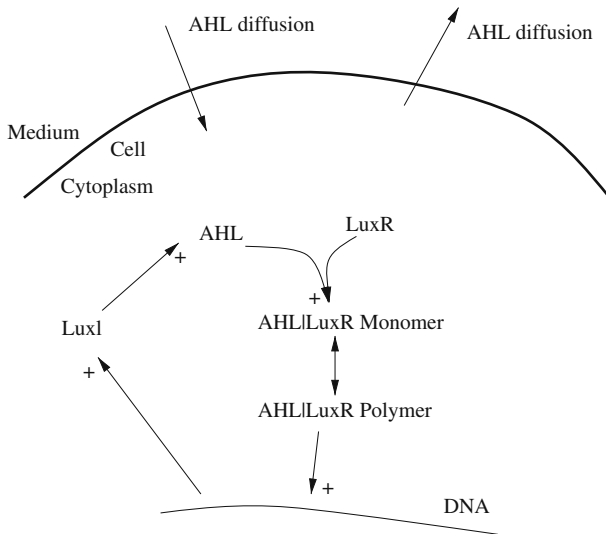


Fig. 1 Scheme of the regulatory pathway

molecules are possible. Most bacteria are regulated by more than one species of signaling molecules (see review articles [3,6]). E.g., *V. fischeri* possesses, apart from the LuxI / LuxR system which utilizes 3OC6HSL, at least one additional signaling pathway, called AinS system. It was shown (e.g., by [11–14]) that this AinS system is, roughly speaking, responsible for the activation of the LuxI / LuxR system. Since this happens at lower cell densities than those we are interested in (direct control of bioluminescence), it is sufficient for our purposes to consider only the LuxI / LuxR system and to neglect the AinS system. A similar simplification was done in the modeling approach in [4] for the species *Pseudomonas aeruginosa*. A putative third system AI-2 which influences luminescence regulation and colonization competence does not play a role here since its influence is small compared to the other systems [11,12] and remains more unspecific.

A sketch of the LuxI / LuxR pathway is given in Fig. 1. LuxI is an enzyme (synthase) that produces AHL at a constant rate (approximately). Under normal conditions, there is a certain background amount of these substances present in the cytoplasm. AHL diffuses into and out of the cell (there is some evidence for an active transport of AHL through the cell membrane; it is very likely that these mechanisms depend on the AHL species [23,30]). In the cytoplasm, it forms a complex with the receptor molecule LuxR. This complex polymerizes to higher clusters. It is then able to act as a transcription factor by binding to the DNA. However, for different LuxR-homologues the details of this process may be different, e.g., it is known that the LuxR-homologue TraR in *Agrobacterium tumefaciens* only dimerizes [30]. The polymer binds to the promoter region of the *lux* operon called *lux*-type box. Here, a variety of genes is activated. Beside those regulating the bioluminescence, also the production of LuxI is increased.

Table 1 Names of variables and parameters for the simplified pathway models

| Variable | Name |
|---|---------------------|
| Mass of AHL outside of the cell | x_e |
| Mass of AHL within the cytoplasm | x_c |
| Parameter | Name |
| Low production rate of AHL | α |
| Increase of production rate of AHL | β |
| Degradation rate of AHL in the cytosol | γ_c |
| Degradation rate of AHL outside of the cell | γ_e |
| Diffusion rate out of the cell of AHL | \tilde{d}_1 |
| Diffusion rate into the cell of AHL | \tilde{d}_2 |
| Threshold of AHL between low and increased activity | x_{thresh} |
| Degree of polymerization | n |

This, in turn increases the rate of AHL production. These processes act as a positive feedback loop. It is well known that this structure may lead to bistability and hysteresis effects [26].

The pathway in Fig. 1 can be described in detail by a system of ordinary differential equations, using the law of mass action, as it is done similarly in [4] for the *las* system. This system of equations for the pathway can be simplified by the introduction of different time scales. Following [4], we assume that all dynamics in the detailed pathway is fast except for that of x_c and x_e .

Hence, we obtain the generic model for QS (for the meaning of variables and parameters see Table 1):

$$\begin{aligned}
 \dot{x}_c &= f(x_c) - \tilde{d}_1 x_c + \tilde{d}_2 x_e, \\
 \dot{x}_e &= \tilde{d}_1 x_c - \tilde{d}_2 x_e - \gamma_e x_e, \\
 f(x_c) &:= \alpha + \frac{\beta x_c^n}{x_{\text{thresh}}^n + x_c^n} - \gamma_c x_c.
 \end{aligned}
 \tag{1}$$

The steady state equation may exhibit one or three (and in non-generic cases also two) nonnegative solutions. Hence, if in the equation for x_c the external signaling substance is assumed to be a (controlled) parameter, we may choose if the cell is resting, activated or if it acts in the bistable regime.

2.2 Between cells: communication via diffusion

We now combine the ODE model of the previous section with spatial structure. We first consider only one cell, assuming the shape of this cell (which can be expected to have only limited influence) to be a ball with radius R centered around the point $x = 0$. We assume furthermore that the concentrations of the substances within the cell are fairly constant w.r.t. space, such that we do not consider a spatially structured model within the cell. Thus, the states within the cell are governed by an ODE (like before), where only the influx/efflux of AHL through the cell membrane need special attention.

Experimental findings seem to suggest that – for a given cell type – there are AHL species that diffuse passively, and others, for which active pumps are located in the cell membrane. Let u_c be the mass of the substance within the cell, $u_e(x)$ the density outside the cell. If we have active pumps, we need to take them into account. We may model this by choosing different rates for inflow and outflow,

$$\text{Net inflow into the cell} = \left(\int_{|x|=R} d_1 u_e(x) - d_2 u_c \, d\sigma \right)$$

and

$$\left(-D \frac{\partial}{\partial \nu} u_e \Big|_{|x|=R} \right) = d_1 u_e(x) - d_2 u_c,$$

where ν denotes the normal of the cell. In case of the simplest model possible, we find

$$\begin{aligned} \frac{d}{dt} u_c &= f(u_c) + \int_{|x|=R} (d_1 u_e(x, t) - d_2 u_c) \, d\sigma \\ \frac{\partial}{\partial t} u_e(x, t) &= D \Delta u_e - \gamma u_e, \\ \left(-D \frac{\partial}{\partial \nu} u_e(x, t) \Big|_{|x|=R} \right) &= d_1 u_e(x, t) - d_2 u_c. \end{aligned}$$

Here, D is the diffusion constant of the signaling substance in the medium outside the cell, and γ corresponds to the degradation rate of the signaling substance. Though in the outer space the density of signaling substance will not change seriously by choosing $\gamma = 0$ instead of a realistic value (about 1/day), mathematically it is desirable to include this term since in this case Hilbert space theory allows to establish necessary *a priori* estimates. In practical applications (Sect. 4), we will choose $\gamma = 0$ nevertheless.

If we have N cells in the system, cell i centered around x_i , then the region in which the signaling substance is defined reads $\Omega = \{x \in \mathbb{R}^3 \mid |x - x_i| > R, 1 \leq i \leq N\}$ and

$$\begin{aligned} \frac{d}{dt} u_c^i &= f(u_c^i) + \int_{|x-x_i|=R} (d_1 u_e(x, t) - d_2 u_c^i) \, d\sigma. \\ \frac{\partial}{\partial t} u_e(x, t) &= D \Delta u_e - \gamma u_e, \\ \left(-D \frac{\partial}{\partial \nu} u_e(x, t) \Big|_{|x-x_i|=R} \right) &= d_1 u_e(x, t) - d_2 u_c^i. \end{aligned} \tag{2}$$

3 Analysis of the model

In this section we will derive useful information about our model. Briefly, we show that stationary solutions are the most interesting solutions, and we will develop a simplified version describing approximatively the stationary solutions of the model. The reduced model only consists of algebraic equations; these are easier to handle than the combination of the partial differential equation and algebraic equations describing the stationary solutions of the original model.

3.1 Dynamical behavior of the model

We investigate some aspects of the dynamics. Taking into account the biological and medical applications, the typical situation is that the system starts subcritical, with low levels of the signaling substance. Slowly the population density grows until the critical density is reached, which leads to a jump to the activated state. Thus, it is of interest to consider the dynamics of the system, starting with low levels of the signaling substance. In the extreme we start with $u_c^i(0) = u_e(x, 0) = 0$.

The system exhibits monotonicity properties: a small amount of signaling substance will increase the production rate that increases the amount of signaling substance and so on. Thus, if we start with a small amount of AHL, the density will monotonously increase in time. Since the density cannot grow unlimited, it finally reaches a steady state. Due to comparison principles (lemma of Nagumo–Westphal), all trajectories starting with non-negative initial conditions below this steady state will finally approach this steady state; one could say that this steady state is stable from below.

This observation gives rise to the introduction of the canonical half-order “ \preceq ” on the state space. Two states $(u_{e,1}(x, t), u_{c,1}^i(t))$ and $(u_{e,2}(x, t), u_{c,2}^i(t))$ are ordered w.r.t. “ \preceq ” at time t , if

$$u_{e,1}(x, t) \leq u_{e,2}(x, t) \text{ a.e.} \quad \text{and} \quad u_{c,1}^i(t) \leq u_{c,2}^i(t).$$

The lemma of Nagumo–Westphal guarantees that two states which are ordered at one point of time stay ordered for all later times.

From our reasoning about the monotonous behavior of solutions with very small initial conditions, we find that the set of all non-negative stationary solutions exhibits a minimal element. A parallel argumentation yields the existence of a maximal element in the set of stationary states that is stable from above. We summarize these results in the following theorem.

Theorem 1 *Let $J_R \subset L^2(\Omega) \times \mathbb{R}^n$ be the set of stationary solutions of the PDE, and \preceq be the canonical half ordering on $L^2(\Omega) \times \mathbb{R}^n$. If $f(x)$ tends to minus infinity for $x \rightarrow \infty$, then J_R is non-empty, has w.r.t. \preceq a minimal element, and all trajectories with initial condition below this minimal element tend asymptotically to this stationary solution. Furthermore, J_R has also a maximal element, and*

all trajectories with initial conditions above this maximal state and asymptotical behavior $u_e(x, t)|_{t=0} \leq C \exp(-\sqrt{\gamma/D}|x|)/|x|$ tend to this maximal state.

(The proof of this theorem is given in Appendix A.) This theorem shows that the set of stationary solutions is quite interesting. All small and all large initial conditions tend to a stationary point. If there is only one stationary point, this point is globally stable (within the set of functions that have an appropriate asymptotic behavior for $|x| \rightarrow \infty$). Based on this theorem, we cannot exclude that there are solutions between the maximal and the minimal element of J_R that oscillate, but we strongly conjecture that there are none and that all solutions eventually tend to a stationary solution. This point of view is the reason for the attempts to gain a deeper understanding of the set J_R . We approach this goal first by investigating the stationary solutions for only one cell. Subsequently, we develop an approximation theorem that allows to state an approximate solution of the PDE. In this way it is possible to reduce the PDE to a set of algebraic equations.

3.2 Stationary solution for one cell

We now aim to describe stationary solutions of this model for one cell only. These considerations are preparations for the following section (the approximation theorem).

Lemma 2 *Consider for $\Omega = \{|x| > R\} \subset \mathbb{R}^3$ the equation*

$$0 = D\Delta u - \gamma u, \quad u|_{|x|=R} = u_0.$$

The unique solution in C^2 that exhibits radial symmetry and vanishes for $r = |x| \rightarrow \infty$ reads

$$U(r) = u_0 \frac{R}{r} e^{-\sqrt{\gamma/D}(r-R)}.$$

Proof Since we look for a classical solution with radial symmetry, we may rewrite the equation in radial coordinates,

$$\frac{d^2}{dr^2}u(r) + \frac{2}{r} \frac{d}{dr}u(r) - \frac{\gamma}{D}u(r) = 0, \quad u(R) = u_0.$$

The general solution of this system reads

$$u(r) = \frac{1}{r} \left[C_1 \sinh(\sqrt{\gamma/D}r) + C_2 \cosh(\sqrt{\gamma/D}r) \right].$$

Since $\sinh(r)$ as well as $\cosh(r)$ tend to infinity for r large, we have necessarily $C_1 = -C_2$, leading to

$$u(r) = \frac{C}{r} e^{-\sqrt{\gamma/D} r}.$$

The constant C is determined by the initial condition. □

Remark 3 In the sense of generalized functions, we find

$$\left(D\Delta - \gamma \right) \frac{1}{|x|} e^{-\sqrt{\gamma/D} |x|} = 4\pi \delta_0(x), \tag{3}$$

i.e., $U(r)$ is the singularity solution of the diffusion operator that is combined with degradation. We will use this fact later in proving an approximation theorem for the stationary solutions.

Remark 4 In equilibrium, we have a defined relation between AHL concentration within the cell and AHL concentration just outside of the cell wall given by the boundary conditions. Since ν is the outer normal of $\{|x| > R\}$ at the boundary $|x| = R$, we find

$$-D \frac{\partial}{\partial \nu} u(x) = D \frac{d}{dr} u(R) = -u_0 \left[\frac{D}{R} + \sqrt{\gamma D} \right]$$

and hence,

$$-u_0 \left[\frac{D}{R} + \sqrt{\gamma D} \right] = d_1 u_0 - d_2 u_c \Rightarrow u_0 = \frac{d_2}{d_1 + D/R + \sqrt{\gamma D}} u_c.$$

Thus, we obtain one single equation for the stationary states of the cell,

$$\begin{aligned} 0 &= f(u_c) + 4\pi R^2 \left[d_1 \frac{d_2}{d_1 + D/R + \sqrt{\gamma D}} u_c - d_2 u_c \right] \\ &= f(u_c) - 4\pi R^2 d_2 \frac{D/R + \sqrt{\gamma D}}{d_1 + D/R + \sqrt{\gamma D}} u_c. \end{aligned}$$

The term $4\pi R^2 d_2 (D/R + \sqrt{\gamma D}) / (d_1 + D/R + \sqrt{\gamma D}) u_c$ obviously describes the net outflow of signaling substance.

Remark 5 This solution allows for certain parameter ranges to be in a bistable mode, i.e. to stay in an activated mode forever, though the cell cannot be activated by a critical population density (there are no other cells). This effect should not play a role in the normal medium, but it may be important, especially if the diffusion rate is changed because the cell is e.g., located in a gel.

3.3 Approximation theorem for stationary solutions

In model (2), cells are treated as objects that extend in the three dimensional space, like they do in realiter. However, cells are quite tiny – it may be possible (and, from the technical point of view, also perhaps desirable) to shrink them to the size of points. I.e., if R denotes the radius of one cell, we are interested in a limit $R \rightarrow 0$ that does only change the solution of $u(x, t)$ up to higher order in R . It is then e.g., possible to find purely algebraic equations for the equilibrium of the population.

First we only consider the signal in the exterior space and develop an approximation for the solution there. We consider N cells, where the region of one cell is $\Omega_i = \{\|x - x_i\| \leq R\}$, $i = 1, \dots, N$. The interior AHL density of cell i is denoted by u_c^i .

In order to consider the asymptotic behavior of the equations for $R \rightarrow 0$, we scale the equations. The scaling behavior of the influx and efflux of a cell is of special interest.

Efflux $u_c^i(t)$ denotes the total mass of signaling substance within cell i . The efflux of the mass is proportional to the surface of the cell, which vanishes with order $\mathcal{O}(R^2)$. Thus, we rescale the proportionality constant of the efflux d_2 by $1/R^2$.

Influx $u_e(x, t)$ is the density of the signaling substance in the medium. We expect point sources to appear in the limit. Thus, close to the center x_i of a cell i , the density behaves like the solution of $D\Delta u + A\delta_{x_i}(x)$, i.e. the density exhibits a pole of order one. Furthermore, the influx is proportional to the cell surface. Altogether, we find that the influx scales according to $\mathcal{O}(1/R) \mathcal{O}(R^2) = \mathcal{O}(R)$. Hence, we rescale the proportionality constant for the influx d_1 by $1/R$. The different scaling of in- and efflux is a consequence of the fact that we consider the mass in the cells, while outside of the cells the density is described.

Rescaled problem: *In the following, we consider the stationary, scaled equation*

$$\begin{aligned}
 0 &= f(u_c^i) + \int_{|x-x_i|=R} \left(\frac{d_1}{R} u_e(x, t) - \frac{d_2}{R^2} u_c^i \right) d\sigma, \\
 0 &= D\Delta u_e - \gamma u_e, \\
 \left(-D \frac{\partial}{\partial \nu} u_e |_{\partial \Omega_i} \right) &= \frac{d_1}{R} u_e - \frac{d_2}{R^2} u_c^i.
 \end{aligned}
 \tag{4}$$

Let $J_R \subset L^2(\Omega) \times \mathbb{R}^n$ be the set of solutions of this equation for given scaling R of the cell radius.

We know the singularity solution of the differential operator [see Eq. (3)]. We expect the solution to be of this form close to a cell. This observation leads to the following definition.

Approximative equations: Let $u_c^i, i = 1, \dots, N$, satisfy the equation

$$0 = f(u_c^i) + \frac{4\pi d_2}{D + d_1} \left\{ - \left(D - d_1 \sqrt{\frac{\gamma}{D}} R \right) u_c^i + R \frac{d_1 D}{(D + d_1)} \sum_{j \neq i} \frac{u_c^j}{\|x_i - x_j\|} \exp \left(-\sqrt{\frac{\gamma}{D}} \|x_i - x_j\| \right) \right\}$$

and define the density $\bar{u}(x)$ by

$$\begin{aligned} \bar{u}(x) &= \sum_{i=1}^N \frac{A_i + R B_i}{\|x - x_i\|} \exp \left(-\sqrt{\frac{\gamma}{D}} \|x - x_i\| \right), \\ A_i &= \exp \left(\sqrt{\frac{\gamma}{D}} R \right) \frac{d_2}{D + d_1 + DR \sqrt{\frac{\gamma}{D}}} \bar{u}_c^i, \\ B_i &= -d_2 d_1 \left(\frac{\exp(\sqrt{\frac{\gamma}{D}} R)}{D + d_1 + DR \sqrt{\frac{\gamma}{D}}} \right)^2 \sum_{j \neq i} \frac{\bar{u}_c^j}{\|x_i - x_j\|} \exp \left(-\sqrt{\frac{\gamma}{D}} \|x_i - x_j\| \right). \end{aligned} \tag{5}$$

Denote with $\tilde{J}_R \subset L^2(\Omega) \times \mathbb{R}^n$ the set of solutions of these equations for given radius R .

The following theorem shows that the rescaled equations and the approximative equations describe essentially the same model. Therefore, we need to define the distance between the sets J_R and \tilde{J}_R . An element $U \in J_R$ is a vector, consisting of the description of the AHL concentration $u(x)$ in the medium and the AHL concentration in the N cells u_c^i . Alike, an element $\tilde{U} \in \tilde{J}_R$ is a vector $(\tilde{u}(x), \tilde{u}_c^i)_{i=1, \dots, N}$. We define as the distance between U and \tilde{U} the distance of the projection to u_c^i resp. \tilde{u}_c^i , since the density within the cells determines the exterior field,

$$\|U - \tilde{U}\| := \max \{ |u_c^i - \tilde{u}_c^i| \mid i = 1, \dots, N \}.$$

The distance between the sets J_R and \tilde{J}_R is now defined in a symmetric way,

$$\begin{aligned} \text{dist}(J_R, \tilde{J}_R) &:= \sup \{ \inf \{ \|U - \tilde{U}'\| \mid \tilde{U}' \in \tilde{J}_R \}, \inf \{ \|U' - \tilde{U}\| \mid U' \in J_R \} \mid U \in J_R, \tilde{U} \in \tilde{J}_R \}. \end{aligned}$$

The proof of the following theorem can be found in Appendix B.

Theorem 6 Consider the stationary, scaled equations (4) resp. the approximative stationary equations (5). Assume $f \in C^2$ is a bounded function and require that the set of nonnegative roots of

$$f(x) - 4\pi \frac{d_1 d_2}{D + d_1} x = 0$$

is finite and

$$f'(x) \neq 4\pi \frac{d_1 d_2}{D + d_1}$$

for any root (i.e. the roots are hyperbolic). Then $\lim_{R \rightarrow 0} J(R) = \lim_{R \rightarrow 0} \tilde{J}(R)$ and there is an $R_0 > 0$, s.t.

$$\text{dist}\{J(R), \tilde{J}(R)\} \leq CR^{3/2} \quad \text{for } 0 \leq R < R_0.$$

Remark 7 (1) Obviously, the communication between cells is a first order term. I.e., if we take the limit $R \rightarrow 0$, the cells are isolated and do not recognize the signals of other cells. This observation may lead to an argument in the discussion QS versus diffusion sensing: a cell that tries primarily to recognize the diffusion coefficient and does not want to communicate with other cells should be small; a cell that wants primarily to communicate should be large. Hence, bacteria that do QS have an evolutionary advantage if they are large, and bacteria that do diffusion sensing have an advantage if they are small. However, the optimal size is of course also determined by many other factors.

(2) The fact that communication depends on R has a technical draw-back: the approximation has only a finite range of validity. If certain magnitudes of R are exceeded, the error explodes. It is even possible that the system does not have any nonnegative solutions. If R is large, or more precisely, if $R/\|x_i - x_j\|$ becomes large, the mass conservation law is not valid any more. The net production of all cells may be less than the amount of signaling substance that the cell receives, i.e.

$$\sum_{i=1}^N u_c^i < \sum_{i=1}^N \sum_{\substack{j=1 \\ j \neq i}}^N \frac{d_1}{D + d_1} \frac{u_c^i}{\|x_i - x_j\|} \frac{R}{\|x_i - x_j\|}.$$

In this case, the approximation breaks down obviously. It is necessary that the spectral bound of the matrix B ,

$$((B))_{i,j} = \begin{cases} -1 & \text{for } i = j \\ \frac{d_1}{(D+d_1)} \frac{R}{\|x_i - x_j\|} & \text{else} \end{cases}$$

is negative. This implies that the distances between the cells have to be much larger than the radius of one cell.

(3) Since only stationary solutions are treated, we do not know anything about the stability of our solutions. However, we expect the eigenvalues of the linearization in our approximative equation to include the information about the stability of the corresponding solutions in the original system.

- (4) Up to now, we considered the cells in a space without obstacles. It is possible, however, to treat a situation where the cells are in a halfspace with homogeneous Dirichlet or Neumann boundary conditions: in order to find a solution, the cells are mirrored at the boundary. For homogeneous Neumann boundary conditions, the mirrored cells are chosen to possess the same state as their originals. The solution of the Dirichlet problem is obtained if the mirrored cells produce the same amount of signaling substance as their original multiplied by minus one. We will use homogeneous Neumann boundary conditions in the next section.

4 Application to image analysis

In this section we demonstrate the application of the theory developed in the present work to the analysis of spatial data obtained by CLSM. This section is intended as an illustrative example only, thus many aspects that are necessary for a profound data analysis are reduced to the absolute minimum.

4.1 Brief description of the biological experiment

Spatial data have been obtained for *Pseudomonas putida* colonizing wheat roots in a monoxenic quartz sand system. *P. putida* produces the AHL N-(3-oxododecanoyl-L-homoserine lactone (3OC12HSL). Two *P. putida* strains were constructed. The AHL producing strain (wild type IsoF, called “producer”) was chromosomally tagged by a *gfp*-gene (green fluorescent protein), which was constitutively expressed [25].

The AHL-deficient detector (called “detector”) strain (F117) contained a plasmid (pKR-C12) bearing a *gfp*-gene regulated by an AHL-controlled promoter [20]. Additionally, it constitutively produced RFP (red fluorescent protein). The expression of GFP in the detector strain reported the presence of a certain amount of AHL at the colonization site. Together with the constitutive RFP labeling, this resulted in a yellow staining of the respective cells, while non-induced cells stayed red. A mixture of producer and detector bacteria was inoculated with the wheat roots in quartz sand containing AHL free plant nutrient medium. This allows the bacteria to colonize the roots up to the development of microcolonies, but without AHL saturation of the medium.

Subsequently, the plant roots were carefully removed, gently washed and excised. The root pieces were transferred to slides. Citifluor (Citifluor Ltd. London, Great Britain) was added to retard fluorescence bleaching. Image stacks of 35 images with 1 μm z -distance were acquired in a CLSM microscope (LSM510, Carl Zeiss, Jena, Germany) with a 40x objective. The software IDL 6.1 (RSI, Boulder, CO, USA) was used to identify bacteria and determine their coordinates. The cells were located in the mucigel layer of the root surface.

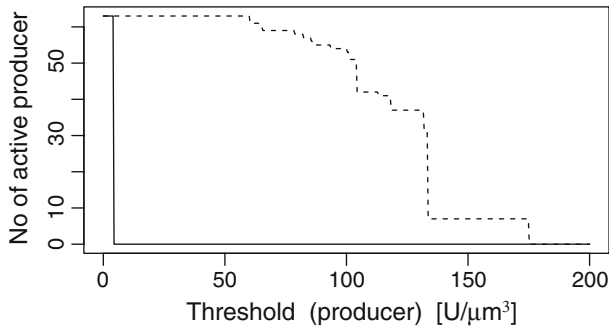


Fig. 2 Number of active producer cells in the minimal (*solid line*) and maximal (*dashed line*) stationary state (see Theorem 3.1) over activation threshold for resting cells. We find a wide parameter region where these two states disagree

4.2 Data analysis

The data are taken from a region of the root which was approximately plain. We model the root surface itself by homogeneous Neumann boundary conditions assuming that the root surface is rather impermeable, and hence approximate the situation by a half-space with a reflecting wall. The degradation of AHL molecules in the outer space plays a minor role (the AHLs have a half-life of about 1 day [22]), which allows us to choose $\gamma = 0$. Thus, we may use “ghost-cells”, i.e. the producer cells are mirrored at the root plain, in order to take the boundary conditions into account.

Producer Since we only know the positions of the producers but not their state, we use the most simple model to characterize these cells: we take the exponent in the Hill function n to infinity, which leads to a step function in the production term. Hence, a producer is “on” or “off”. In the less active “resting” state (cell is “off”) the producer synthesizes AHL molecules with a certain low rate. We normalize the units and choose this production rate to 1U per time unit. From [25] we know that the production rate of activated cells is around 100 times higher than that of resting cells. The only unknown parameter of the producer is the threshold at which cells switch between activated and resting state. This needs to be determined in the course of data analysis.

If the threshold is given, we are able to determine the minimal and the maximal state (similar to theorem 1). In Fig. 2 we draw the number of active cells for the minimal and maximal resting state over the threshold. We find a wide parameter range for bi- and multiple stability. In the following, we only consider the maximal resting state; this restriction, however, is arbitrary and has to be removed in a profound data analysis.

Detector From the detector cells we know locations and activity. Since we have more detailed informations, we are able to use a refined model (in comparison to the model of the producer). Given the AHL concentration at the location of the detector cell, we predict the probability that this cell is active by a logit

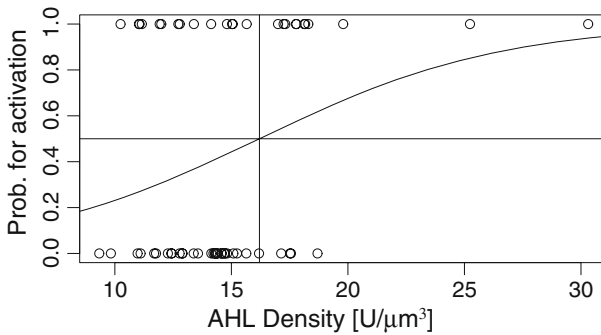


Fig. 3 Probability for a detector cell to become activated over AHL density. The *line* denotes the prediction of the logit model, while the *dots* denote the resting cells (dot at $p = 0$) resp. the activated cells (dot at $p = 1$)

model. This choice allows (via generalized linear models) a fast computation of parameters and of the log-likelihood.

Result of the analysis Altogether, we need to determine three parameters: the threshold of the producer and two parameters for the logit model. Maximizing the likelihood, we find the most appropriate parameter set with respect to the given data. For the optimal parameters, the plot of the probability to be an activated detector versus AHL density is shown in Fig. 3. The prediction of the state of the cells resp. the AHL density is shown in Fig. 4. We find a small cluster of seven producers in the center that are active. Basically, they determine the AHL density. All other producer cells are predicted to be in the resting state.

This example shows that the model and the approximation theorem developed in the present paper can be used to analyze spatial data about individual cells. Nevertheless, in this example we simplified and neglected effects; the most important ones are: consideration of the maximal stationary state only, possible loss of the ability of the detector cells to become activated, boundary effects, the importance of stationary states that are neither the maximal nor the minimal state. However, using this technique in a more sophisticated way, it will be possible to do single cell analysis and to reveal information e.g. about communication distances and intercellular variability.

5 Discussion

In the present work the theoretical background for the analysis of data that allow conclusions about location and state of single cells is developed. This aim is reached in four steps: first, we present a model for cell–cell communication by QS. This model is based on the standard approaches for this phenomenon, and extends them to the description of single cells embedded in the three-dimensional space. The system consists of a linear, parabolic partial differential equation that describes the diffusion of signaling substance coupled with

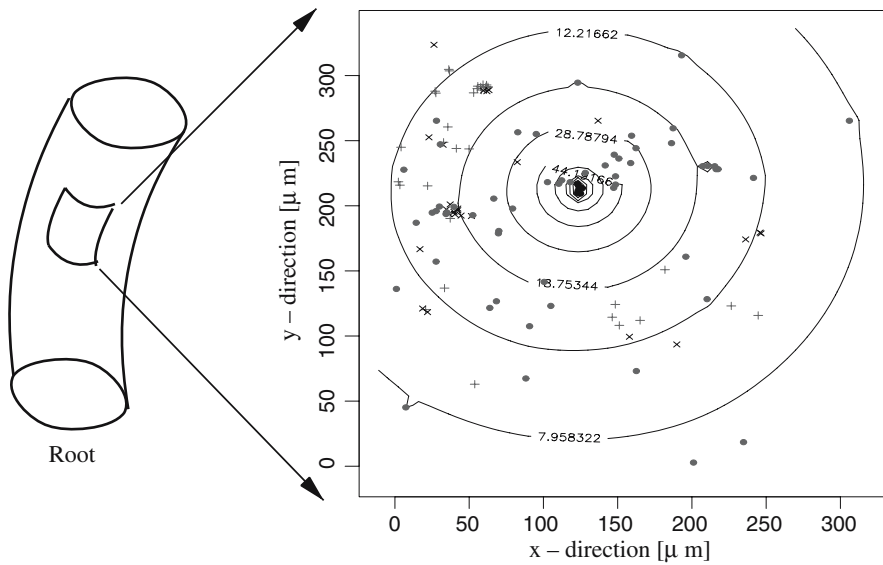


Fig. 4 Plot of the spatial data. *Circles* denote the measured location of producers. These circles are *black* if the model predicts activation (this is only the case for a cluster of seven cells in the center of the picture) while *grey dots* represent resting producer cells. *Plus signs* mark the measured location of resting, *cross signs* that of active detector cells. The *equipotential lines* denote the density of AHL concentration predicted by the model (normalized units)

ordinary differential equations describing the state of the regulatory network within the cells.

In the second step, we exploit the fact that the system is cooperative. We basically find that trajectories tend to stationary states. This fact seems to agree with experimental findings, where the states of the cells do not change after a primary transient phase. This finding gives rise to take a closer look on the set of stationary states.

In the third step we develop a method to simplify the equations describing the stationary states: one problem (for the analysis as well as for numerical approaches) is the fact that cells are expanded objects in space. However, considering the size of cells with respect to their distance, cells are quite tiny. They may be regarded as point sources of signaling substances. Rescaling arguments translate this idea into a mathematical setting. The resulting partial differential equation can be solved explicitly s.t. we obtain a finite system of purely algebraic equations for the states of the cells. These simplified equations allow a fast numerical computation of the state of the system, which is necessary to perform the last step – the image analysis. Moreover, these equations reveal that a cell primarily is influenced by its own signal, measuring the diffusion coefficient close to its location. The interaction with other cells is a second order term. This finding contributes to the discussion “QS” against “diffusion sensing”: primarily, the cell does diffusion sensing. The QS is a higher order term. Nevertheless, this term may be the one governing the system if the parameters are chosen in

such a way that – under normal conditions, i.e. a normal diffusion coefficient in the neighborhood of the cell – the own signal is a kind of background calibration of the system.

The last step in the present work is the application of this formalism to data obtained by CLSM. Though only intended as an illustration of the applicability of the theory developed above, one may recognize that in this way useful information can be obtained from these data. Especially an idea about the activation threshold and communication distances may be revealed. In order to do this in a proper way, however, especially the statistical model that tells us the probability for a cell to be fluorescent at a given density of signaling substances needs to be refined in order to take into account the subtlety of the experiment (e.g., cells may loose their fluorescence gene).

Acknowledgments We thank Karsten Rodenacker who kindly performed the image analysis of the data.

Appendix A: Dynamical behavior of the model

In order to prove Theorem 1, we need two propositions.

Proposition 8 *Consider the system*

$$\begin{aligned} \frac{d}{dt}u_c^i &= f(u_c^i) + \int_{|x-x_i|=R} (d_1u_e(x,t) - d_2u_c^i) \, do \\ \frac{\partial}{\partial t}u_e(x,t) &= D\Delta u_e - \gamma u_e, \\ \left(-D \frac{\partial}{\partial v}u_e(x,t) \Big|_{|x-x_i|=R}\right) &= d_1u_e(x,t) - d_2u_c^i \end{aligned}$$

with initial conditions

$$u_e|_{t=0} = 0, \quad u_c^i(0) = 0.$$

The solution is non-decreasing in t.

Proof If $f(0) = 0$, the solution reads $u_e(x,t) = u_c^i(t) = 0$, and the proposition is true. Hence, we may assume that $f(0) > 0$. Following the usual scheme of proofs of this type (see e.g. [27]), we slightly change the differential equations and consider

$$\begin{aligned} \frac{d}{dt}u_{c,\epsilon}^i &= f(u_{c,\epsilon}^i) + \epsilon t + \int_{|x-x_i|=R} (d_1u_{e,\epsilon}(x,t) - d_2u_{c,\epsilon}^i) \, d\sigma \\ \frac{\partial}{\partial t}u_{e,\epsilon}(x,t) &= D\Delta u_{e,\epsilon} - \gamma u_{e,\epsilon}, \\ \left(-D\frac{\partial}{\partial \nu}u_{e,\epsilon}(x,t)\Big|_{|x-x_i|=R}\right) &= d_1u_{e,\epsilon}(x,t) - d_2u_{c,\epsilon}^i. \end{aligned}$$

In this case, there is a first time interval $(0, t_1)$, where $\dot{u}_{c,\epsilon}^i(t) > 0$. For $\partial_t u_{e,\epsilon}(x, t) =: v_\epsilon(x, t)$, we obtain the partial differential equation (first considering the difference quotient $(u(x, t + h) - u(x, t))/h$, then taking the limit $h \rightarrow 0$)

$$\begin{aligned} \frac{\partial}{\partial t}v_\epsilon(x,t) &= D\Delta v_\epsilon - \gamma v_\epsilon, \\ \left(-D\frac{\partial}{\partial \nu}v_\epsilon(x,t)\Big|_{|x-x_i|=R}\right) &= d_1v_\epsilon(x,t) - d_2\dot{u}_{c,\epsilon}^i. \end{aligned}$$

Since $\dot{u}_{c,\epsilon}^i(t) > 0$, we find as a consequence of the lemma of Nagumo–Westphal that $v_\epsilon(x, t) \geq \hat{v}_\epsilon(x, t)$, where \hat{v}_ϵ satisfies

$$\begin{aligned} \frac{\partial}{\partial t}\hat{v}_\epsilon(x,t) &= D\Delta \hat{v}_\epsilon - \gamma \hat{v}_\epsilon, \\ \left(-D\frac{\partial}{\partial \nu}\hat{v}_\epsilon(x,t)\Big|_{|x-x_i|=R}\right) &= d_1\hat{v}_\epsilon(x,t), \\ \hat{v}_\epsilon(x,0) &= v_\epsilon(x,0) = \partial_t u_{e,\epsilon}(x,t)|_{t=0} = 0 \end{aligned}$$

(see e.g. [27, Corollar V, p.224]). Since $\hat{v}_\epsilon(x, t) = 0$, $v_\epsilon(x, t)$ is nonnegative as long as $\dot{u}_{c,\epsilon}^i(t) \geq 0$ for all $i = 1, \dots, N$.

Now assume that there is a first time point t_1 and $i_0 \in \{1, \dots, N\}$ s.t. $\dot{u}_{c,\epsilon}^{i_0}(t_1) = 0$, $\dot{u}_{c,\epsilon}^{i_0}(t_1 + \delta) < 0$ for $\delta > 0$ and δ sufficiently small. Then

$$\begin{aligned} \ddot{u}_{c,\epsilon}^{i_0}(t_1) &= f'(u_{c,\epsilon})\dot{u}_{c,\epsilon}^{i_0}(t_1) + \epsilon + \int_{|x-x_{i_0}|=R} (d_1v_\epsilon(x,t) - d_2\dot{u}_{c,\epsilon}^{i_0}) \, d\sigma \\ &\geq \epsilon > 0. \end{aligned}$$

Thus, for δ positive and sufficiently small, we have $\dot{u}_{c,\epsilon}^{i_0}(t_1) < 0$, which is a contradiction to the assumption that t_1 is the first time point where the monotonicity is broken.

Since the solution of the PDE depends continuously on the right hand side, we may let $\epsilon \rightarrow 0$ and obtain the desired result. □

Proposition 9 Consider the system

$$\begin{aligned} \frac{d}{dt}u_c^i &= f(u_c^i) + \int_{|x-x_i|=R} (d_1u_e(x,t) - d_2u_c^i) \, do \\ \frac{\partial}{\partial t}u_e(x,t) &= D\Delta u_e - \gamma u_e \\ \left(-D \frac{\partial}{\partial \nu} u_e(x,t) \Big|_{|x-x_i|=R}\right) &= d_1u_e(x,t) - d_2u_c^i. \end{aligned}$$

Let $f(x) + \beta N < 0$ for $x > x_0$ and consider the initial conditions $u_c^i(0) = u_0^i > x_0$, $u_e(x, 0) = u_{e,0}(x)$, where $u_{e,0}(x)$ satisfies the elliptic problem

$$\begin{aligned} 0 &= D\Delta u_{e,0} - \gamma u_{e,0}, \\ \left(-D \frac{\partial}{\partial \nu} u_{e,0}(x) \Big|_{|x-x_i|=R}\right) &= d_1u_{e,0}(x) - d_2u_0^i. \end{aligned}$$

Then, the solution is non-increasing in time.

Proof The proof follows exactly the proof of the last lemma; the only thing is to see that the function $v(x, t) = 0$ for $t = 0$ due to the special choice of the initial condition for u_e . □

Now we are ready to prove Theorem 1.

Proof (of Theorem 1) First we show that the solution of the PDE for zero initial conditions asymptotically tends to a stationary point. We already know that the solution is non-decreasing. Since $f(\cdot)$ becomes eventually negative, we know that $u_c^i(t)$ are bounded. Thus, these functions tend to a stationary point. Hence, also $u_e(x, t)$ becomes stationary, the solution of the system tends to $(u_c^{i*}, u_e^*(x)) \in J$ and thus J is non-empty. By the comparison principle that is a consequence of the Nagumo–Westphal lemma, all trajectories with nonnegative initial conditions below this stationary point tend to this stationary point. Hence, there may be no other stationary points below $(u_c^{i*}, u_e^*(x))$, this is the minimal element of J , indeed.

The same arguments hold true for the maximal state. We need to control the asymptotics in order to find a suited initial condition that forms a super solution of a trajectory under consideration. □

Appendix B: Approximation theorem

In this section, we essentially prove Theorem 6. In order to derive this proof, we need several propositions and lemmata.

B.1 Equation for the residual

Lemma 10 Consider the scaled equation

$$0 = D\Delta u - \gamma u, \quad \left(-D \frac{\partial}{\partial \nu} u \Big|_{\partial \Omega_i}\right) = \frac{d_1}{R} u - \frac{d_2}{R^2} a_i$$

and the function

$$\bar{u}(x) = \sum_{i=1}^N \frac{A_i + RB_i}{\|x - x_i\|} \exp\left(-\sqrt{\frac{\gamma}{D}} \|x - x_i\|\right),$$

where A_i and B_i are given by

$$A_i = \exp\left(\sqrt{\frac{\gamma}{D}} R\right) \frac{d_2}{D + d_1 + DR\sqrt{\frac{\gamma}{D}}} a_i, \quad B_i = -d_2 d_1 \left(\frac{\exp(\sqrt{\frac{\gamma}{D}} R)}{D + d_1 + DR\sqrt{\frac{\gamma}{D}}}\right)^2 \sum_{j \neq i} \frac{a_j}{\|x_i - x_j\|} \exp\left(-\sqrt{\frac{\gamma}{D}} \|x_i - x_j\|\right).$$

Let $v(x)$ be defined by

$$u(x) = \bar{u}(x) + v(x).$$

For $v(x)$, we obtain

$$0 = D\Delta v - \gamma v \quad \left(-D \frac{\partial}{\partial \nu} v \Big|_{\partial \Omega_{i_0}}\right) - \frac{d_1}{R} v = g_{i_0}(x; R).$$

The function $g_{i_0}(x; R)$ has an in R uniform $L^\infty(\partial \Omega_{i_0})$ -bound and reads

$$\begin{aligned} g_{i_0}(x; R) = & -\frac{d_1}{R} \sum_{i \neq i_0} A_i \frac{\|x - x_i\| \exp(\sqrt{\frac{\gamma}{D}} \|x - x_i\|) - \|x_{i_0} - x_i\| \exp(\sqrt{\frac{\gamma}{D}} \|x_{i_0} - x_i\|)}{\|x - x_i\| \|x_{i_0} - x_i\| \exp(\sqrt{\frac{\gamma}{D}} \|x - x_i\|) \exp(\sqrt{\frac{\gamma}{D}} \|x_{i_0} - x_i\|)} \\ & + D \sum_{i \neq i_0} \frac{A_i + RB_i}{R} \exp\left(-\sqrt{\frac{\gamma}{D}} \|x - x_i\|\right) \\ & \times \left[\frac{1}{\|x - x_i\|^3} + \sqrt{\frac{\gamma}{D}} \frac{1}{\|x - x_i\|^2} \right] (x - x_{i_0})^T (x - x_i) \\ & + d_1 \sum_{i \neq i_0} B_i \frac{1}{\|x - x_i\|} \exp\left(-\sqrt{\frac{\gamma}{D}} \|x - x_i\|\right). \end{aligned}$$

Proof First of all, $\nabla\|x - x_i\| = (x - x_i)/\|x - x_i\|$. Thus, with $V_i = A_i + RB_i$,

$$\nabla\bar{u} = \sum_{i=1}^N V_i \cdot \exp\left(-\sqrt{\frac{\gamma}{D}}\|x - x_i\|\right) \cdot \left[\frac{-(x - x_i)}{\|x - x_i\|^3} - \sqrt{\frac{\gamma}{D}} \frac{x - x_i}{\|x - x_i\|^2}\right]$$

and $D\Delta\bar{u} - \gamma\bar{u} = 0$. The outer normal for $x \in \partial\Omega_{i_0}$ reads $\nu(x) = (x_{i_0} - x)/\|x_{i_0} - x\|$. Hence,

$$\begin{aligned} \frac{\partial}{\partial \nu}\bar{u}|_{\partial\Omega_{i_0}} &= \nu^T(x) \nabla\bar{u}(x) \\ &= \frac{-(x - x_{i_0})^T}{\|x - x_{i_0}\|} \\ &\quad \times \left(\sum_{i=1}^N V_i \cdot \exp\left(-\sqrt{\frac{\gamma}{D}}\|x - x_i\|\right) \cdot \left[\frac{-(x - x_i)}{\|x - x_i\|^3} - \sqrt{\frac{\gamma}{D}} \frac{x - x_i}{\|x - x_i\|^2}\right]\right) \\ &= V_{i_0} \exp\left(-\sqrt{\frac{\gamma}{D}}R\right) \cdot \left[\frac{1}{R^2} + \frac{1}{R}\sqrt{\frac{\gamma}{D}}\right] \\ &\quad + \sum_{i \neq i_0} V_i \exp\left(-\sqrt{\frac{\gamma}{D}}\|x - x_i\|\right) \\ &\quad \times \left[\frac{1}{\|x - x_i\|^3} + \sqrt{\frac{\gamma}{D}} \frac{1}{\|x - x_i\|^2}\right] \frac{(x - x_{i_0})^T(x - x_i)}{R}. \end{aligned}$$

Now we use the ansatz $u = \bar{u} + v$ and $V_i = A_i + RB_i$. Plugging this ansatz into the boundary conditions and collecting for terms of the same powers of R yields

$$\begin{aligned} &\left(-D \frac{\partial}{\partial \nu} v|_{\partial\Omega_{i_0}}\right) \\ &= \left(-D \frac{\partial}{\partial \nu} u|_{\partial\Omega_{i_0}}\right) - \left(-D \frac{\partial}{\partial \nu} \bar{u}|_{\partial\Omega_{i_0}}\right) \\ &= \frac{d_1}{R}(\bar{u}(x) + v(x))|_{\partial\Omega_{i_0}} - \frac{d_2}{R^2}a_{i_0} + DV_{i_0} \exp\left(-\sqrt{\frac{\gamma}{D}}R\right) \cdot \left[\frac{1}{R^2} - \frac{1}{R}\sqrt{\frac{\gamma}{D}}\right] \\ &\quad + D \sum_{i \neq i_0} V_i \exp\left(-\sqrt{\frac{\gamma}{D}}\|x - x_i\|\right) \cdot \left[\frac{1}{\|x - x_i\|^3} - \sqrt{\frac{\gamma}{D}} \frac{1}{\|x - x_i\|^2}\right] \\ &\quad \times \frac{(x - x_{i_0})^T(x - x_i)}{R} \\ &= D \frac{A_{i_0}}{R^2} \exp\left(-\sqrt{\frac{\gamma}{D}}R\right) - \frac{d_2}{R^2}a_{i_0} + \frac{d_1}{R^2}A_{i_0} \exp\left(-\sqrt{\frac{\gamma}{D}}R\right) + \frac{d_1}{R}v \\ &\quad + D \frac{B_{i_0}}{R} \exp\left(-\sqrt{\frac{\gamma}{D}}R\right) + \frac{d_1}{R}B_{i_0} \exp\left(-\sqrt{\frac{\gamma}{D}}R\right) \end{aligned}$$

$$\begin{aligned}
 &+ \frac{d_1}{R} \sum_{i \neq i_0} A_i \frac{1}{\|x_{i_0} - x_i\|} \exp\left(-\sqrt{\frac{\gamma}{D}} \|x_{i_0} - x_i\|\right) \\
 &- \frac{d_1}{R} \sum_{i \neq i_0} A_i \frac{\|x - x_i\| \cdot \exp(\sqrt{\frac{\gamma}{D}} \|x - x_i\|) - \|x_{i_0} - x_i\| \cdot \exp(\sqrt{\frac{\gamma}{D}} \|x_{i_0} - x_i\|)}{\|x - x_i\| \cdot \|x_{i_0} - x_i\| \cdot \exp(\sqrt{\frac{\gamma}{D}} \|x - x_i\|) \cdot \exp(\sqrt{\frac{\gamma}{D}} \|x_{i_0} - x_i\|)} \\
 &- D \frac{A_{i_0}}{R} \exp\left(-\sqrt{\frac{\gamma}{D}} R\right) \sqrt{\frac{\gamma}{D}} - DB_{i_0} \exp\left(-\sqrt{\frac{\gamma}{D}} R\right) \sqrt{\frac{\gamma}{D}} \\
 &+ D \sum_{i \neq i_0} (A_i + RB_i) \cdot \exp\left(-\sqrt{\frac{\gamma}{D}} \|x - x_i\|\right) \cdot \left[\frac{1}{\|x - x_i\|^3} - \sqrt{\frac{\gamma}{D}} \frac{1}{\|x - x_i\|^2}\right] \\
 &\times \frac{(x - x_{i_0})^T (x - x_i)}{R} \\
 &+ d_1 \sum_{i \neq i_0} B_i \frac{1}{\|x - x_i\|} \exp\left(-\sqrt{\frac{\gamma}{D}} \cdot \|x - x_i\|\right).
 \end{aligned}$$

The basic idea is now to collect terms of same order of R . However, it turns out that slightly more intuitive results can be obtained, if we do not expand the exponential functions and if we include one term of order minus one in the equation that otherwise only takes care of terms of order minus two. We thus require

$$\begin{aligned}
 &DA_{i_0} \exp\left(-\sqrt{\frac{\gamma}{D}} R\right) - d_2 a_{i_0} + d_1 A_{i_0} \exp\left(-\sqrt{\frac{\gamma}{D}} R\right) \\
 &+ DA_{i_0} R \exp\left(-\sqrt{\frac{\gamma}{D}} R\right) \sqrt{\frac{\gamma}{D}} = 0,
 \end{aligned}$$

which is satisfied by the choice above for A_i . Similarly, we consider the terms of order minus one (excluding terms where the residual $v(x)$ appears),

$$\begin{aligned}
 &DB_{i_0} \exp\left(-\sqrt{\frac{\gamma}{D}} R\right) + d_1 B_{i_0} \exp\left(-\sqrt{\frac{\gamma}{D}} R\right) + DB_{i_0} R \exp\left(-\sqrt{\frac{\gamma}{D}} R\right) \sqrt{\frac{\gamma}{D}} \\
 &= - \sum_{i \neq i_0} A_i \frac{d_1}{\|x_{i_0} - x_i\|} \cdot \exp\left(-\sqrt{\frac{\gamma}{D}} \|x_{i_0} - x_i\|\right).
 \end{aligned}$$

This equation determines the choice of B_i . Thus, $v(x)$ fulfills the PDE given above.

We show now that there is a uniform L^∞ bound for $g_i(x; R)$ for $x \in \partial\Omega_i$. Since $g(x; R)$ is continuous and $\partial\Omega_i$ is compact, for $R > 0$, fixed, there is such a bound. The only problem that may appear is that this bound blows up for $R \rightarrow 0$. The first and the second sum contain R^{-1} , i.e. could be unbounded. If we consider

the first sum, we find

$$\begin{aligned} & \frac{d_1}{R} \sum_{i \neq i_0} A_i \frac{\|x - x_i\| \exp(\sqrt{\frac{\gamma}{D}} \|x - x_i\|) - \|x_{i_0} - x_i\| \exp(\sqrt{\frac{\gamma}{D}} \|x_{i_0} - x_i\|)}{\|x - x_i\| \|x_{i_0} - x_i\| \exp(\sqrt{\frac{\gamma}{D}} \|x - x_i\|) \exp(\sqrt{\frac{\gamma}{D}} \|x_{i_0} - x_i\|)} \\ &= \sum_{i \neq i_0} \frac{g_a(\|x - x_i\|) - g_a(\|x_{i_0} - x_i\|)}{R} \\ & \quad \times \frac{d_1 A_i}{\|x - x_i\| \|x_{i_0} - x_i\| \exp(\sqrt{\frac{\gamma}{D}} \|x - x_i\|) \exp(\sqrt{\frac{\gamma}{D}} \|x_{i_0} - x_i\|)}, \end{aligned}$$

where $g_a(x) = x \exp(\sqrt{\frac{\gamma}{D}} x)$. Since $g_a(x)$ is differentiable in x and $x \rightarrow x_{i_0}$ for $R \rightarrow 0$, we obtain

$$\frac{g_a(x - x_i) - g_a(x_{i_0} - x_i)}{R} = \frac{\mathcal{O}(R)}{R} = \mathcal{O}(R^0),$$

i.e. this term is bounded. Similarly, for the second sum we have

$$\begin{aligned} & \left\| D \sum_{i \neq i_0} \frac{A_i + RB_i}{R} \exp\left(-\sqrt{\frac{\gamma}{D}} \|x - x_i\|\right) \left[\frac{1}{\|x - x_i\|^3} + \sqrt{\frac{\gamma}{D}} \frac{1}{\|x - x_i\|^2} \right] \right. \\ & \quad \times (x - x_{i_0})^T (x - x_i) \left. \right\| \leq D \sum_{i \neq i_0} \frac{A_i + RB_i}{R} \exp\left(-\sqrt{\frac{\gamma}{D}} \|x - x_i\|\right) \\ & \quad \times \left[\frac{1}{\|x - x_i\|^3} + \sqrt{\frac{\gamma}{D}} \frac{1}{\|x - x_i\|^2} \right] \|x - x_{i_0}\| \|x - x_i\|. \end{aligned}$$

Since $\|x - x_{i_0}\| = R$, this term is also uniformly bounded in R . □

B.2 Existence of weak solutions

In order to prove that the residual function $v(x)$ tends to zero for $R \rightarrow 0$, we first define the weak solution of the equation for v , and then show existence of the solution and investigate the asymptotic behavior of the H^1 and the L^2 norm for $R \rightarrow 0$.

Problem 11 Let $x \in \Omega, \Omega = \mathbb{R}^n \setminus (\cup_{i=1}^N \Omega_i)$, where Ω_i are bounded regions with C^∞ -boundary. Consider the elliptic equation

$$\begin{aligned} & -D \Delta v + \gamma v = 0, \\ & \left(-D \frac{\partial}{\partial \nu} v |_{\partial \Omega_i} \right) - av = g(x; R), \end{aligned}$$

where

$$\|g(x; R)\|_{L^\infty(\partial\Omega)} \leq g_\infty < \infty, \quad D, \gamma, a > 0.$$

Remark 12 (1) In order to derive the usual definition of weak solutions in a heuristic way, we assume that a solution $u(x)$ of this equation is smooth and nice. Multiplying the solution with a function Φ (that is also assumed to be as nice as necessary) we find

$$\begin{aligned} 0 &= \int_{\Omega} \Phi(x)(-D\Delta u(x)) \, dx + \gamma \int_{\Omega} \Phi(x)u(x) \, dx \\ &= D \int_{\Omega} \nabla \Phi(x)\nabla u(x) \, dx + \int_{\partial\Omega} \Phi(x) \left(-D \frac{\partial}{\partial \nu} u(x)\right) \, d\sigma + \gamma \int_{\Omega} \Phi(x)u(x) \, dx \\ &= D \int_{\Omega} \nabla \Phi(x)\nabla u(x) \, dx + \int_{\partial\Omega} \Phi(x)(a \nu(x) + g(x; R)) \, d\sigma + \gamma \int_{\Omega} \Phi(x)u(x) \, dx. \end{aligned}$$

(2) In the expression above an integral over $\partial\Omega$ appears. However, we will control the H^1 norm of u . With the L^2 norm and the H^1 norm, we also have an estimate for the norm of the Besov space $B^{1/2,2,1}$. Though Ω is an unbounded region, $\partial\Omega = \cup_{i=1}^N \partial\Omega_i$ is bounded (and smooth). Hence, the trace operator

$$T : B^{1/2,2,1}(\Omega) \rightarrow L^2(\partial\Omega)$$

is linear and continuous, i.e. bounded [1, Theorem 7.43 and Remark 7.45],

$$\|Tu\|_{L^2(\partial\Omega)} \leq C\|u\|_{B^{1/2,2,1}(\Omega)} \leq C'\|u\|_{H^1(\Omega)}.$$

Below, we will use $\|T\| = \|T\|_{L^2(\partial\Omega), H^1(\Omega)}$. For $u \in H^1$, we find the interpolation inequality

$$\|u\|_{B^{1/2,2,1}(\Omega)} \leq t^{-\theta} \max\{\|u\|_{L^2(\Omega)}, t\|u\|_{H^1(\Omega)}\}$$

with $\theta = 1/2$ and $t > 0$ arbitrarily [1, Lemma 7.19 and Paragraph 7.32].

Definition 13 For $u, v \in H^1(\Omega)$ define

$$\begin{aligned} B[u, v] &= \int_{\Omega} D\nabla u(x) \nabla v(x) \, dx + a \int_{\partial\Omega} (Tv)(x)(Tu)(x) \, d\sigma + \gamma \int_{\Omega} v(x)u(x) \, dx \\ F[v] &= - \int_{\partial\Omega} (Tv)(x)g(x; R) \, d\sigma, \end{aligned}$$

where $T : H^1(\Omega) \rightarrow L^2(\partial\Omega)$ denotes the trace operator. If $u \in H^1(\Omega)$ satisfies

$$B[u, v] = F[v] \quad \forall v \in H^1(\Omega),$$

we call $u(x)$ a weak solution of the partial differential equation introduced in Problem 11.

Proposition 14 *The bilinear form $B : H^1(\Omega) \times H^1(\Omega) \rightarrow \mathbb{R}$ is coercive,*

$$\begin{aligned} |B[u, v]| &\leq c_1 \|u\|_{H^1(\Omega)} \|v\|_{H^1(\Omega)}, \\ B[u, u] &\geq c_2 \|u\|_{H^1(\Omega)}^2, \end{aligned}$$

where $c_1 = \gamma + D + a \|T\|^2$ and $c_2 = \min\{\gamma, D\}$. The linear form $F : H^1(\Omega) \rightarrow \mathbb{R}$ is bounded,

$$|F[v]| \leq g_\infty \sqrt{|\partial\Omega|} \|T\| \|v\|_{H^1(\Omega)}.$$

Proof The boundedness of $F[\cdot]$ is a consequence of the boundedness of the trace operator T ,

$$\begin{aligned} |F[v]| &\leq g_\infty \int_{\partial\Omega} |(Tv)(x)| \, d\sigma \leq g_\infty \left(\int_{\partial\Omega} 1^2 \, d\sigma \right)^{1/2} \left(\int_{\partial\Omega} |(Tv)(x)|^2 \, d\sigma \right)^{1/2} \\ &\leq g_\infty \sqrt{|\partial\Omega|} \|T\| \|v\|_{H^1(\Omega)}. \end{aligned}$$

The first estimate for $B[u, v]$ follows again from the continuity of the trace operator,

$$\begin{aligned} |B[u, v]| &\leq D \|\nabla u\|_{L^2(\Omega)} \|\nabla v\|_{L^2(\Omega)} + \gamma \|u\|_{L^2(\Omega)} \|v\|_{L^2(\Omega)} + a \|Tu\|_{L^2(\partial\Omega)} \|Tv\|_{L^2(\partial\Omega)} \\ &\leq (D + \gamma + a \|T\|^2) \|u\|_{H^1(\Omega)} \|v\|_{H^1(\Omega)}. \end{aligned}$$

The second estimate for $B[u, u]$ essentially needs $\gamma, a > 0$,

$$\begin{aligned} B[u, u] &= \int_{\Omega} D |\nabla u(x)|^2 \, dx + a \int_{\partial\Omega} |(Tu)(x)|^2 \, d\sigma + \gamma \int_{\Omega} |u(x)|^2 \, dx \\ &\geq \min\{D, \gamma\} \|u\|_{H^1(\Omega)}^2. \end{aligned}$$

□

Theorem 15 *The partial differential equation defined in Problem 11 has a unique weak solution $u \in H^1(\Omega)$ with*

$$\|u\|_{H^1(\Omega)} \leq \frac{g_\infty \|T\|}{\min\{D, \gamma\}} \sqrt{|\partial\Omega|}.$$

The $L^2(\Omega)$ norm of this solution can be bounded by

$$\|u\|_{L^2(\Omega)} \leq C|\partial\Omega|.$$

Proof The proof of the existence and the $H^1(\Omega)$ estimate of the weak solution follows immediately from our last proposition together with the Lax–Milgram–Theorem [19].

We now prove the $L^2(\Omega)$ bound. From $B[u, u] = F[u]$ we obtain

$$\begin{aligned} - \int_{\partial\Omega} (Tu)(x)g(x; R) \, d\sigma &= \int_{\Omega} D|\nabla u(x)|^2 \, dx + a \int_{\partial\Omega} |(Tu)(x)|^2 \, d\sigma + \gamma \int_{\Omega} |u(x)|^2 \, dx \\ \Rightarrow \gamma \|u\|_{L^2(\Omega)}^2 &\leq - \int_{\partial\Omega} (Tu)(x)g(x; R) \, d\sigma - \int_{\Omega} D|\nabla u(x)|^2 \, dx \\ &\quad - a \int_{\partial\Omega} |(Tu)(x)|^2 \, d\sigma \\ &\leq \int_{\partial\Omega} |(Tu)(x)| |g(x; R)| \, d\sigma \\ &\leq \|g(x; R)\|_{L^\infty(\partial\Omega)} \int_{\partial\Omega} |(Tu)(x)| \, d\sigma \\ &\leq C \|u\|_{H^1(\Omega)} \sqrt{|\partial\Omega|} \leq C' |\partial\Omega|. \end{aligned}$$

□

Remark 16 (1) In our application, we have $|\partial\Omega| = \mathcal{O}(R^2)$, where R denotes the radius of the cells. Thus, we find that the H^1 norm of the solution is of first and the L^2 norm of second order in R .

(2) Due to the trace theorem and the interpolation inequality for Besov spaces, we find immediately

$$\begin{aligned} \|v\|_{L^1(\partial\Omega)} &\leq \|u\|_{L^2(\partial\Omega)} \|1\|_{L^2(\partial\Omega)} \leq \|u\|_{B^{1/2,2,1}(\Omega)} \sqrt{|\partial\Omega|} \\ &\leq C t^{-1/2} \max\{\|u\|_{L^2(\Omega)}, t\|u\|_{H^1(\Omega)}\} R. \end{aligned}$$

If we choose $t = R$, we have

$$\|v\|_{L^1(\partial\Omega)} \leq C R^{-1/2} \max\{C' R^2, C'' R^2\} R = \mathcal{O}(R^{5/2}).$$

Corollary 17 Let $u(x)$ and $\bar{u}(x)$ be defined as in Lemma 10. Then

$$u(x) = \bar{u}(x) + v(x),$$

where for R sufficiently small

$$\|v\|_{L^2(\Omega)} \leq CR^2, \quad \|v\|_{H^1(\Omega)} \leq CR, \quad \|v\|_{L^1(\partial\Omega)} \leq CR^{5/2}.$$

B.3 Error estimates

Up to now, we investigated the exterior region. We now focus rather on the interior of the cells, where the nonlinearity is located at. In order to be able to describe the effect of the exterior field on the cells, we first make the linearity of feedback and interaction via the external field more explicit.

Lemma 18 *Let $(u_c^i)_{i=1,\dots,n}$ and $u(x)$ satisfy the Eqs. (4) and $(\bar{u}_c^i)_{i=1,\dots,n}$ and $\bar{u}(x)$ satisfy the approximative Eqs. (5). Let the vectors u_c and \bar{u}_c be $u_c = (u_c^1, \dots, u_c^N)^T$, $u_c = (\bar{u}_c^1, \dots, \bar{u}_c^N)^T$. We then define maps M, \bar{M} and \tilde{M} that depend on R , $M = M(R)$, and $\bar{M} = \bar{M}(R)$ and $\tilde{M} = \tilde{M}(R)$, by*

$$\begin{aligned} \bar{M} : \mathbb{R}^N &\rightarrow \mathbb{R}^N \\ u_c &\mapsto \left(\frac{4\pi d_2}{D + d_1} \left\{ - \left(D - d_1 \sqrt{\frac{\gamma}{D}} R \right) u_c^i \right. \right. \\ &\quad \left. \left. + R \frac{d_1 D}{(D + d_1)} \sum_{j \neq i} \frac{u_c^j}{\|x_i - x_j\|} \exp \left(-\sqrt{\frac{\gamma}{D}} \|x_i - x_j\| \right) \right\} \right)_{i=1,\dots,N} \end{aligned}$$

$$M : \mathbb{R}^N \rightarrow \mathbb{R}^N$$

$$u_c \mapsto \left(\frac{d_1}{R} \int_{|x-x_i|=R} u(x) \, d\sigma - \frac{d_2}{R^2} \int_{|x-x_i|=R} u_c^i \, d\sigma \right)_{i=1,\dots,N}$$

$$\tilde{M} : \mathbb{R}^N \rightarrow \mathbb{R}^N$$

$$\bar{u}_c \mapsto \left(\frac{d_1}{R} \int_{|x-x_i|=R} \bar{u}(x) \, d\sigma - \frac{d_2}{R^2} \int_{|x-x_i|=R} \bar{u}_c^i \, d\sigma \right)_{i=1,\dots,N}.$$

We find

$$\begin{aligned} \tilde{M}(R) &= \bar{M}(R) + \mathcal{O}(R^2), \\ M(R) &= \tilde{M}(R) + \mathcal{O}(R^{3/2}) = \bar{M}(R) + \mathcal{O}(R^{3/2}). \end{aligned}$$

Proof First of all, given $(u_c^i)_{i=1,\dots,N}$, the exterior field u depends in a linear manner on these constants. I.e., $M(R)$, $\bar{M}(R)$ and $\tilde{M}(R)$ can be written as matrices. Since we know $\bar{u}(x)$ explicitly [see Eq. (5)], we are able to evaluate the integrals up to first order. Because of

$$\frac{1}{4\pi R} \int_{|x-x_i|=R} \frac{\exp\left(-\sqrt{\frac{\gamma}{D}}\|x-x_i\|\right)}{\|x-x_j\|} \, d\omega = \begin{cases} 1 - \sqrt{\frac{\gamma}{D}}R + \mathcal{O}(R^2) & \text{if } i = j \\ R \frac{\exp\left(-\sqrt{\frac{\gamma}{D}}\|x_i-x_j\|\right)}{\|x_i-x_j\|} + \mathcal{O}(R^2) & \text{for } i \neq j \end{cases},$$

we find

$$\begin{aligned} (\tilde{M}(R)\bar{u}_c)_i &= \frac{d_1}{R} \int_{|x-x_i|=R} \bar{u}(x) \, d\omega - \frac{d_2}{R^2} \int_{|x-x_i|=R} u_c^i \, d\omega \\ &= 4\pi \left\{ d_1(A_i + RB_i) \left(1 - \sqrt{\frac{\gamma}{D}}R\right) \right. \\ &\quad \left. + d_1 \sum_{j \neq i} A_j R \frac{\exp\left(-\sqrt{\frac{\gamma}{D}}\|x_i-x_j\|\right)}{\|x_i-x_j\|} - d_2 \bar{u}_c^i + \mathcal{O}(R^2) \right\} \\ &= 4\pi \left\{ \frac{d_2 d_1}{D + d_1} \bar{u}_c^i \left(1 - \sqrt{\frac{\gamma}{D}}R\right) \right. \\ &\quad - R \frac{d_2 d_1^2}{(D + d_1)^2} \sum_{j \neq i} \frac{\bar{u}_c^j}{\|x_i-x_j\|} \exp\left(-\sqrt{\frac{\gamma}{D}}\|x_i-x_j\|\right) \\ &\quad + d_1 \sum_{j \neq i} \frac{d_2}{D + d_1} R \frac{\bar{u}_c^j}{\|x_i-x_j\|} \exp\left(-\sqrt{\frac{\gamma}{D}}\|x_i-x_j\|\right) \\ &\quad \left. - d_2 \bar{u}_c^i + \mathcal{O}(R^2) \right\} \\ &= 4\pi \left\{ -d_2 \frac{D - d_1 \sqrt{\frac{\gamma}{D}}R}{D + d_1} \bar{u}_c^i + R \frac{d_2 d_1 D}{(D + d_1)^2} \right. \\ &\quad \left. \times \sum_{j \neq i} \frac{\bar{u}_c^j}{\|x_i-x_j\|} \exp\left(-\sqrt{\frac{\gamma}{D}}\|x_i-x_j\|\right) + \mathcal{O}(R^2) \right\} \\ &= (\bar{M}(R)\bar{u}_c)_i + \mathcal{O}(R^2). \end{aligned}$$

Thus, $\bar{M}(R) = \tilde{M}(R) + \mathcal{O}(R^2)$. Furthermore, we have (if we define $v(x)$ by $u(x) = \bar{u}(x) + v(x)$)

$$\left\| (M(R)a)_i - (\tilde{M}(R)a)_i \right\| = \left| \frac{1}{R} \int_{\|x-x_i\|=R} v(x; R) \, d\omega \right| \leq \frac{1}{R} \|v\|_{L^1(\partial\Omega)} = \mathcal{O}(R^{3/2}).$$

Hence, $M(R) = \tilde{M}(R) + \mathcal{O}(R^{3/2}) = \bar{M}(R) + \mathcal{O}(R^2) + \mathcal{O}(R^{3/2}) = \bar{M}(R) + \mathcal{O}(R^{3/2})$. □

Remark 19 (1) Equations (4) and (5) can be written as

$$\begin{aligned} f(u_c^i) + (M(R)u_c)_i &= 0 \\ f(\bar{u}_c^i) + (\bar{M}(R)\bar{u}_c)_i &= 0. \end{aligned}$$

(2) All functions $M(R)$, $\tilde{M}(R)$ and $\bar{M}(R)$ are continuously differentiable: for $\bar{M}(R)$ and $\tilde{M}(R)$, this is a direct consequence of the representation. For $M(R)$, it can be shown by transforming Ω using smooth functions, s.t. the holes $\{|x - x_i| \leq R\}$ become $\{|x - x_i| \leq 1\}$. These transformations yield (smooth) inhomogeneities and coefficients in the PDE. Since the solution of an elliptic PDE depends smoothly on the coefficients, also M depends smoothly on R .

Now we are able to prove the approximation Theorem 6.

Proof (of Theorem 6) First of all, we find from $M(R)$, $\bar{M}(R)$ and $\tilde{M}(R)$ considered in the last lemma,

$$M(R) \rightarrow \tilde{M}(0), \quad \bar{M}(R) \rightarrow \tilde{M}(0).$$

Since f is bounded, the set of all positive solutions of $f(a_i) + (\tilde{M}(R)a)_i = 0$ resp. $f(a_i) + (\bar{M}(R)a)_i = 0$ is a subset of a compact set. Furthermore, $f \in C^2$. Thus, for a small interval in R , this set stays finite and hyperbolic. Therefore, $J(R)$ as well as $\tilde{J}(R)$ tend to the set of solutions of $f(a_i) + (\tilde{M}(0)a)_i = 0$, we have

$$J(0) = \tilde{J}(0).$$

The estimate of the distance between $J(R)$ and $\tilde{J}(R)$ can be shown by a contraction principle. Due to the hyperbolicity and differentiability of the approximative equations, we may apply the implicit function theorem and find that (for each vector in $\tilde{J}(0)$) there is a family $\bar{u}_c(R) = (u_c^1(R), \dots, u_c^N(R))^T$ that solves the approximative problem for $0 \leq R < R_0$, R_0 sufficiently small. Now we consider the ansatz

$$u_c(R) = \bar{u}_c(R) + \Delta(R) \in \mathbb{R}^n,$$

i.e. the function $\Delta(R)$ denotes the difference between $u_c(R)$ and $\bar{u}_c(R)$. We derive a fixed point equation for $\Delta(R)$ that shows that there are $u_c(R) \in \mathbb{R}^n$ which solve the original problem and $\|\Delta(R)\| = \mathcal{O}(R^{3/2})$.

We find (if we interpret $f(u_c)$ as $(f(u_c^1), \dots, f(u_c^N))^T$ etc.)

$$\begin{aligned} 0 &= f(\bar{u}_c(R) + \Delta(R)) + M(R)(\bar{u}_c(R) + \Delta(R)) \\ &= f(\bar{u}_c(R) + \Delta(R)) + \bar{M}(R)(\bar{u}_c(R) + \Delta(R)) + (M(R) - \bar{M}(R))(\bar{u}_c(R) + \Delta(R)) \\ &= f(\bar{u}_c(R)) + f'(\bar{u}_c(R))\Delta(R) + \mathcal{O}(\|\Delta(R)\|^2) + \bar{M}(R)\bar{u}_c(R) + \bar{M}(R)\Delta(R) \\ &\quad + (M(R) - \bar{M}(R))\bar{u}_c(R) + (M(R) - \bar{M}(R))\Delta(R) \end{aligned}$$

$$= \left(f'(\bar{u}_c(R)) + \bar{M}(R) \right) \Delta(R) + \mathcal{O}(R^{3/2}) + \mathcal{O}(R^{3/2}) \Delta(R) + \mathcal{O}(\|\Delta(R)\|^2).$$

Since $\tilde{J}(0)$ is hyperbolic, for $f'(\bar{u}_c(R)) + \bar{M}(R)$ there is an inverse if $0 \leq R < R_0$, if R_0 is chosen small enough. Hence,

$$\Delta(R) = [f'(\bar{u}_c(R)) + \bar{M}(R)]^{-1} \left(\mathcal{O}(R^{3/2}) + \mathcal{O}(R^{3/2}) \Delta(R) + \mathcal{O}(\|\Delta(R)\|^2) \right).$$

We furthermore know that $\Delta(0) = 0$. Consider

$$B_{R_0,\epsilon} := \{ \varphi \in C^0[0, R_0] \mid \varphi(0) = 0, \quad \|\varphi\|_{C^0[0,R_0]} \leq \epsilon \}$$

and

$$\begin{aligned} \mathcal{T} : B_{R_0,\epsilon} \rightarrow C^0, \quad \varphi \mapsto & [f'(\bar{u}_c(R)) + \bar{M}(R)]^{-1} \\ & \times \left(\mathcal{O}(R^{3/2}) + \mathcal{O}(R^{3/2}) \varphi(R) + \mathcal{O}(\|\varphi(R)\|^2) \right). \end{aligned}$$

It is straight forward to see that – for R_0 and ϵ small – \mathcal{T} maps $B_{R_0,\epsilon}$ into itself and is, moreover, a contraction in $B_{R_0,\epsilon}$. Thus, there is a unique solution. For this solution we find

$$\|\Delta(R)\| \leq \|\mathcal{T}\| \left(\mathcal{O}(R^{3/2}) + \mathcal{O}(\|\Delta(R)\|^2) \right)$$

and thus

$$\|\Delta(R)\| = \mathcal{O}(R^{3/2}).$$

This proves that $R^{3/2}$ -close to any point in $\tilde{J}(R)$, there is a point in $J(R)$.

The other direction (for any point in $J(R)$, there is a point $\tilde{J}(R)$ that is $\mathcal{O}(R^{3/2})$ -close) follows with similar arguments. □

References

1. Adams, R., Fournier, J.: Sobolev Spaces. Elsevier, Amsterdam (2003)
2. Bassler, B.: How bacteria talk to each other: regulation of gene expression by quorum sensing. *Curr. Opin. Microbiol.* **2**, 582–587 (1999)
3. Daniels, R., Vanderleyden, J., Michiels, J.: Quorum sensing and swarming migration in bacteria. *FEMS Microbiol. Rev.* **28**, 261–289 (2004)
4. Dockery, J., Keener, J.: A mathematical model for quorum sensing in *Pseudomonas aeruginosa*. *Bull. Math. Biol.* **63**, 95–116 (2001)
5. Eberhard, A., Burlingame, A., Eberhard, C., Kenyon, G., Nealson, K., Oppenheimer, N.: Structural identification of autoinducer of *Photobacterium fischeri* luciferase. *Biochemistry* **20**, 2444–2449 (1981)
6. Fuqua, C., Greenberg, P.E.: Listening on bacteria: acyl-homoserine lactone signalling. *Nat. Rev.* **3**, 685–695 (2002)

7. Gantner, S.: Mikrobielle Ökologie N-Acyl-L-Homoserinlacton-produzierender Bakterien in der Rhizosphäre von Tomatenpflanzen. PhD Thesis, Ludwig-Maximilian-Universität München (2003)
8. Gray, K., Greenberg, E.: Physical and functional maps of the luminescence gene cluster in an autoinducer-deficient *Vibrio fischeri* strain isolated from a squid light organ. *J. Bacteriol.* **174**, 4384–4390 (1992)
9. Kaplan, H., Greenberg, E.: Diffusion of autoinducers is involved in regulation of the *Vibrio fischeri* luminescence system. *J. Bacteriol.* **163**, 1210–1214 (1985)
10. Koerber, A., King, J., Williams, P.: Deterministic and stochastic modelling of endosome escape by *Staphylococcus aureus*: “quorum” sensing by a single bacterium. *J. Math. Biol.* **50**, 440–488 (2005)
11. Kuo, A., Blough, N., Dunlap, P.: Multiple N-acyl-L-homoserine lactone autoinducers of luminescence in the marine symbiotic bacterium *Vibrio fischeri*. *J. Bacteriol.* **176**, 7558–7565 (1994)
12. Lupp, C., Ruby, E.: *Vibrio fischeri* LuxS and AinS: comparative study of two signal synthases. *J. Bacteriol.* **186**, 3873–3881 (2004)
13. Lupp, C., Ruby, E.: *Vibrio fischeri* uses two quorum-sensing systems for the regulation of early and late colonization factors. *J. Bacteriol.* **187**, 3620–3629 (2005)
14. Lupp, C., Urbanowski, M., Greenberg, E., Ruby, E.: The *Vibrio fischeri* quorum-sensing systems *ain* and *lux* sequentially induce luminescence gene expression and are important for persistence in the squid host. *Mol. Microbiol.* **50**, 319–331 (2003)
15. Miller, M., Bassler, B.: Quorum sensing in bacteria. *Annu. Rev. Microbiol.* **55**, 165–199 (2001)
16. Nealson, K., Platt, T., Hastings, J.: Cellular control of the synthesis and activity of the bacterial luminescent system. *J. Bacteriol.* **104**, 313–322 (1970)
17. Ravn, L., Christensen, A., Molin, S., Givskov, M., Gram, L.: Methods for detecting acylated homoserine lactones produced by Gram-negative bacteria and their application in studies of AHL-production kinetics. *J. Microbiol. Methods* **44**, 239–251 (2001)
18. Redfield, R.J.: Is quorum sensing a side effect of diffusion sensing? *Trends Microbiol.* **10**, 365–370 (2002)
19. Renardy, M., Rogers, R.C.: *An Introduction to Partial Differential Equations*. Springer, Berlin Heidelberg New York (1992)
20. Riedel, K., Hentzer, M., Geisenberger, O., Huber, B., Steidle, A., Wu, H., Hoiby, N., Givskov, M., Molin, S., Eberl, L.: N-acylhomoserine-lactone-mediated communication between *Pseudomonas aeruginosa* and *Burkholderia cepacia* in mixed biofilms. *Microbiology* **147**, 3249–3262 (2001)
21. Ruby, E., Lee, K.-H.: The *Vibrio fischeri*-*Euprymna scolopes* light organ association: current ecological paradigms. *Appl. Environ. Microbiol.* **64**(3), 805–812 (1998)
22. Schaefer, A., Val, B., Hanzelka, B., Cronan, J., Greenberg, E.: Detection, purification and structural elucidation of acylhomoserine lactone inducer of *Vibrio fischeri* luminescence and other related molecules. *Method. Enzymol.* **305**, 288–301 (2000)
23. Sharma, A., Sahgal, M., Johri, B.: Microbial communication in the rhizosphere: operation of quorum sensing. *Curr. Sci.* **85**, 1164–1172 (2003)
24. Steidle, A., Sigl, K., Schuhegger, R., Ihring, A., Schmid, M., Gantner, S., Stoffels, M., Riedel, K., Givskov, M., Hartmann, A., Langebartels, C., Eberl, L.: Visualization of N-Acylhomoserine lactone-mediated cell-cell communication between bacteria colonizing the tomato rhizosphere. *Appl. Environ. Microbiol.* **67**, 5761–5770 (2001)
25. Steidle, A., Allesen-Holm, M., Riedel, K., Berg, G., Givskov, M., Molin, S., Eberl, L.: Identification and characterization of an N-Acylhomoserine Lactone-dependent quorum-sensing system in *Pseudomonas putida* strain IsoF. *Appl. Environ. Microbiol.* **68**, 6371–6382 (2002)
26. Thyson, J., Othmer, H.: The dynamics of feedback control circuits in biochemical pathways. *Progr. Theor. Biol.* **5**, 1–62 (1978)
27. Walter, W.: *Differential- und Integral- Ungleichungen*. Springer, Berlin Heidelberg New York (1964)
28. Ward, J., King, J., Koerber, A., Croft, J., Socket, R., Williams, P.: Cell-signalling repression in bacterial quorum sensing. *Math. Med. Biol.* **21**, 169–204 (2004)
29. Waters, C., Bassler, B.: Quorum sensing: Cell-to-cell communication in bacteria. *Annu. Rev. Cell. Dev. Biol.* **21**, 319–346 (2005)
30. Whitehead, N., Barnard, A., Slater, H., Simpson, N., Salmond, G.: Quorum-sensing in Gram-negative bacteria. *FEMS Microbiol. Rev.* **25**, 365–404 (2001)
31. You, L., Cox R.S. III, Weiss, R., Arnold, F.A.: Programmed population control by cell-cell communication and regulated killing. *Nature* **428**, 868–871 (2004)